

# Radiative Heating in Scramjet Combustors

H. F. Nelson\*

University of Missouri–Rolla, Rolla, Missouri 65409-0050

Currently, there is considerable interest in scramjet engines for hypersonic aircraft and missiles. This paper presents preliminary calculations of the radiative heating of the walls of scramjet combustion chambers. The analysis assumes isothermal, constant property flowfields that are representative of actual combustor flowfields. The fuel is  $H_2$ , and  $N_2$  is taken as inert. Temperature in the combustor is on the order of 2000–3000 K and the pressure is of the order of 5 atm. The combustion products consist mainly of  $H_2O$  and  $OH$ . These gases are strong radiators in the infrared. Radiation heating can be significant because of high temperature and pressure and the strong gas emission. The radiation fluxes from  $H_2O$  and  $OH$  are predicted to be as large as  $24 \text{ W/cm}^2$ , depending on the size of the combustor. Larger combustors have larger radiative heating. Radiation heating is roughly 10% of the convective heating. For airplane applications, where the engine must go through many cycles between overhauls, the combustor will need thermal radiative protection.

## Nomenclature

$A$	= parameter, Eq. (1)
$a$	= fine structure parameter
$CD$	= collisional-Doppler optical depth
$d$	= line spacing, $1/\text{cm}$
$E$	= activation energy, $\text{kJ/gmol}$
$F(0)$	= radiative flux, $\text{W/cm}^2$
$F_\omega(0)$	= spectral radiative flux, $\text{W}/(\text{cm}^2\text{-sr-}1/\text{cm})$
$h_{aw}$	= adiabatic wall enthalpy, $\text{kJ/kg}$
$h_w$	= combustor wall enthalpy, $\text{kJ/kg}$
$I_B$	= blackbody intensity, $\text{W}/(\text{cm}^2\text{-sr-}1/\text{cm})$
$I_\omega$	= radiative intensity, $\text{W}/(\text{cm}^2\text{-sr-}1/\text{cm})$
$K_{eq}$	= equilibrium constant
$k_b$	= backward reaction rate, $\text{gmol}/(\text{cm}^3\text{-s})$
$k_f$	= forward reaction rate, $\text{gmol}/(\text{cm}^3\text{-s})$
$L$	= length, $\text{cm}$
$M$	= Mach number
$M_w$	= molecular weight, $\text{kg/kmol}$
$N$	= exponent, Eq. (1)
$P$	= pressure, $\text{atm}$
$\dot{q}$	= convective heat transfer rate, $\text{W/cm}^2$
$R_u$	= gas constant, $8.314 \text{ kJ}/(\text{kmol-K})$
$S/d$	= line strength to half-width ratio, $1/\text{cm}$
$St$	= Stanton number, $\approx 0.01$
$s$	= path length, $\text{cm}$
$T$	= temperature, $\text{K}$
$u$	= pseudothickness, $\text{cm}$
$v$	= velocity, $\text{m/s}$
$X$	= band model optical depth
$x, y, z$	= coordinate directions, Fig. 2
$Y$	= mole fraction
$\gamma$	= line half-width, $1/\text{cm}$
$\eta$	= parameter for line half-width, Eq. (16)
$\theta$	= polar angle, $\text{deg}$
$\kappa_\omega$	= absorption coefficient, $1/\text{cm}$
$\rho$	= density, $\text{kg/m}^3$
$\tau_\omega$	= optical depth

$\phi$	= equivalence ratio, or azimuthal angle, $\text{deg}$
$\omega$	= wave number, $1/\text{cm}$

## Subscripts

$C$	= collisional
$i, j$	= gas $i$ , gas $j$
$k$	= reaction $k$
$p$	= calculation point
$0$	= freestream condition, combustor size

## Superscript

*	= Beer's law
---	--------------

## Introduction

**S**UPERSONIC combustion ramjet (scramjet) engines are being developed for future hypersonic vehicles. Both NASA and the U.S. Air Force have research programs to develop propulsion systems and airframes that could evolve into hypersonic missiles and aircraft.<sup>1</sup> The U.S. Air Force program expects to develop a practical engine that could be used in Mach 4–8 hypersonic missile applications by 2002. NASA's Hyper-X program involves demonstrating analytic methods, conducting wind-tunnel tests, and flying a 12-ft-long, unmanned, scramjet-powered aircraft in the Mach 6–10 range. These engines must be analyzed to determine their combustion characteristics with respect to mission parameters, such as pressure, temperature, Mach number, angle of attack, and fuel–air ratio.

Scramjet engines are not without operational tradeoffs. Fuel–air mixing by diffusion in the high-speed flow is limited because of the short residence times. In conventional ramjet engines decelerating the air required for combustion to subsonic speeds entails enormous losses. In scramjets high inlet flow velocities, flameholding and ignition delay require long combustion chambers. Combustion chambers can be made shorter using mixing enhancement strategies, but at the expense of thrust losses.<sup>2</sup>

Scramjet combustors operate at temperatures in the 2000–3000 K range and the combustion products are good radiators. Radiation heat transfer predictions are necessary to determine how much thermal protection must be used on the combustor walls. This is especially important for airplanes, because they must operate for long periods of time and over many takeoff and landing cycles without engine refurbishment.

Large-scale ramjet/scramjet tests are being planned at NASA Langley Research Center, focusing on developing the technology necessary for air-breathing hypersonic vehicles.<sup>3</sup> Goals of

Presented as Paper 96-1843 at the AIAA 31st Thermophysics Conference, New Orleans, LA, June 17–20, 1996; received June 28, 1996; accepted for publication Sept. 11, 1996. Copyright © 1996 by the American Institute of Aeronautics and Astronautics, Inc. All rights reserved.

\*Professor of Aerospace Engineering, Thermal Radiative Transfer Group, Department of Mechanical and Aerospace Engineering and Engineering Mechanics. Associate Fellow AIAA.

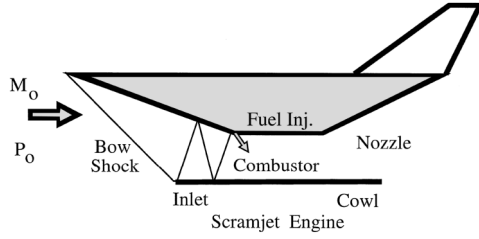


**Fig. 1** Schematic of a scramjet powered vehicle showing details of the engine.

the test are to explore scale effects on combustor efficiency, thrust, boundary-layer development, and drag within the engine.

The supersonic combustion ramjet (scramjet) is shown schematically in Fig. 1. It uses a diffusive-type inlet to decelerate the incoming air, and increase the air temperature and pressure. Figure 1 shows the bow shock, the oblique shock waves in the engine inlet, and the fuel injection. The lower aft surface of the vehicle serves as the engine nozzle. The inlet oblique shock waves lead to high combustion chamber temperatures and pressures (2000–3000 K and 1–5 atm, respectively).<sup>4</sup> For  $H_2$  fuel the combustion products are mainly  $H_2O$  and  $OH$ . These gases are strong radiation emitters at temperatures from 2000 to 3000 K. Consequently, radiative heating of the combustion chamber walls may be important, not only because of high temperatures and pressures, but also because of strong gas emission.

Liu and Tiwari<sup>5</sup> investigated the radiative and conductive heating of scramjet nozzle walls. They used an iteration procedure to solve the Navier–Stokes equations with a Monte Carlo analysis to calculate the  $H_2O$  radiation. The radiation calculations were done using a narrow-band model for the  $H_2O$  spectra. Results are presented for several hydrogen–air equivalence ratios, wall temperatures, inlet temperatures, and nozzle sizes. In general, they show that radiative heating ranges from 20 to 50 W/cm<sup>2</sup>, which is 2–10 times larger than the conductive heating.

The objective of this research is to present a preliminary analysis of radiative heating on scramjet combustor walls. The spectral variation of the gas radiative emission is accurately modeled. The research is done with a simple, but representative flowfield. The results of this research serve as an indication of the importance of radiative heating in scramjet combustors.

### Combustion Modeling

The computer code SPARK, developed at NASA Langley Research Center, was used to make calculations of  $H_2$ –air combustion flowfields in scramjet combustor configurations at Mach 14. SPARK is a compressible Navier–Stokes code intended specifically for reacting flow problems. The code was originally developed by Drummond et al.<sup>6,7</sup> Explicit details of the code structure, implementation, and accuracy are given in Refs. 6–9. Additional scramjet combustor solutions at Mach 9.77 and 7.67 were obtained using a generic, cycle-code based on the quasi-one-dimensional stream-tube theory (Refs. 10 and 11).

The chemistry model considered seven species ( $H_2$ ,  $O_2$ ,  $N_2$ ,  $H_2O$ ,  $H$ ,  $O$ , and  $OH$ ), and seven reactions, which is consistent with the system used by Singh et al.,<sup>8</sup> and a subset of the system used by Drummond et al.<sup>7</sup>  $N_2$  was assumed to be inert. The forward chemical reaction rate is

$$k_{f_k} = A_k T^{N_k} \exp(-E_k/R_u T) \quad (1)$$

The values of  $A$  [for  $k_{f_i} = \text{cm}^3/(\text{gmol}\cdot\text{s})$  for two-body reactions,  $\text{cm}^6/(\text{gmol}^2\cdot\text{s})$  for three-body reactions],  $N$  (unitless), and  $E$  (kJ/gmol) are given in Table 1. The reverse rate is

$$k_{b_k} = k_{f_k}/K_{eq,k} \quad (2)$$

### Radiation Transport

Assume the combustor is a volume of radiating gas bounded by plane walls as shown in Fig. 2. The gas is assumed to be isothermal and to have constant properties. The general equation of transfer in the region is

$$\frac{dI_\omega(\tau_\omega, \theta, \phi)}{d\tau_\omega} + I_\omega(\tau_\omega, \theta, \phi) = I_B(\omega, T) \quad (3)$$

where  $\tau_\omega = \kappa_\omega s$ , and where  $s$  is a function of  $\theta$  and  $\phi$ . The medium is assumed to be nonscattering. The radiation intensity at  $z = 0$  for any  $x$  and  $y$  is of interest here, and so this equation has the general solution<sup>12</sup>

$$I_\omega(0, \theta, \phi) = I_\omega(\tau_{0\omega}, \theta, \phi) \exp(-\tau_{0\omega}) + \int_0^{\tau_{0\omega}} I_B(\omega, t) \exp(-t) dt \quad (4)$$

where

$$\tau_{0\omega} = \kappa_\omega s_0 \quad (5)$$

and  $s_0$  is a function of  $\theta$  and  $\phi$ .  $s_0$  represents the distance along the intensity vector to the boundary. The first and second terms on the right-hand side of Eq. (4) represent the radiation from the wall at distance  $\tau_{0\omega}$  and from the gas, respectively.

Equation (4) must be integrated over the entire solid angle to account for all of the radiation reaching a point on the wall at  $z = 0$ . The solid angle is  $\sin \theta d\theta d\phi$ , where  $\theta$  ranges from 0 to  $\pi/2$ , and  $\phi$  is the azimuthal angle and ranges from 0 to  $2\pi$ :

$$F_\omega(0) = \int_0^{2\pi} \left[ \int_0^{\pi/2} I_\omega(0, \theta, \phi) \cos \theta \sin \theta d\theta \right] d\phi \quad (6)$$

This equation, when integrated over all wave numbers, gives the radiative flux to the combustor walls

$$F(0) = \int_0^\infty F_\omega(0) d\omega \quad (7)$$

The infrared radiation absorption coefficients for the combustion gases are evaluated using the band model methods of

**Table 1** Radiation rate data

Reaction	$A$	$N$	$E$
$H_2 + O_2 \rightleftharpoons OH + OH$	$1.70 \times 10^{13}$	0.0	201.5
$H + O_2 \rightleftharpoons OH + O$	$1.42 \times 10^{14}$	0.0	68.60
$OH + H_2 \rightleftharpoons H_2O + H$	$3.16 \times 10^7$	1.8	12.78
$O + H_2 \rightleftharpoons OH + H$	$2.07 \times 10^{14}$	0.0	57.50
$OH + OH \rightleftharpoons H_2O + O$	$5.50 \times 10^{13}$	0.0	29.30
$H + OH + M \rightleftharpoons H_2O + M$	$2.21 \times 10^{22}$	-2	0.00
$H + H + M \rightleftharpoons H_2 + M$	$6.53 \times 10^{17}$	-1	0.00

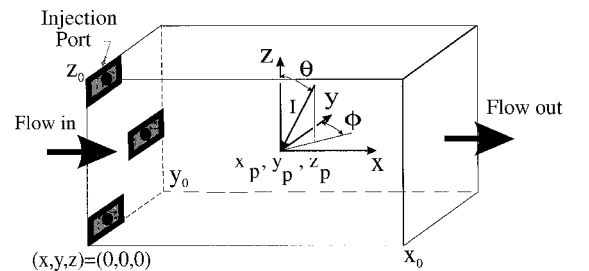


**Fig. 2** Schematic of a scramjet combustor, showing the radiation geometry. View is from underneath the combustor, such that  $x$  = length,  $y$  = height, and  $z$  = width.

Ref. 13. References 13–15 contain data for several diatomic and triatomic combustion product molecules.

### Molecular Band Modeling

Molecular band modeling is used to determine  $\tau_\omega$  for the radiation calculations. This section follows the development on pages 220 and 221 of Ref. 13.  $X_i$  is given by

$$X_i = [1 - (1/\sqrt{CD_i})]X_i^* \quad (8)$$

The parameter  $CD_i$  is the combined collisional and Doppler optical depth. Since the combustor temperature is of the order of 2000–3000 K, and the combustor pressure is of the order of 5 atm, Doppler effects are not important. Consequently,  $CD_i$  is given by

$$CD_i = [1 - (X_{Ci}/X_i^*)^2]^{-2} \quad (9)$$

The optical depth in the weak line limit (Beer's law optical depth) is

$$X_i^* = \int_0^{u_i} \kappa_{\omega i} du' \quad (10)$$

where  $u_i$  is at standard temperature and pressure (STP)

$$u_i = Y_i P(273/T)L \quad (11)$$

where  $L$  is the path length given by

$$L = \sqrt{(x - x_p)^2 + (y - y_p)^2 + (z - z_p)^2} \quad (12)$$

The temperature ratio converts the data to STP. The absorption coefficient  $\kappa_{\omega i}$  of gas  $i$  is given by

$$\kappa_{\omega i} = (S/d)_i (273/T) Y_i P, \quad 1/\text{cm} \quad (13)$$

where  $(S/d)_i$  is a function of  $\omega$  and  $T$ . It is tabulated for the molecules of interest.<sup>13</sup> Values of  $(S/d)$  are also available from the SRRM database.<sup>14,15</sup>

The optical depth for a pure collision curve of growth is

$$X_{Ci} = X_i^* \frac{1}{[1 + X_i^*/(4a_{Ci})]^{1/2}} \quad (14)$$

where  $a_{Ci}$  is the collision-broadened fine structure parameter:

$$a_{Ci} = \frac{1}{X_i^*} \int_0^{u_i} \left( \frac{\gamma_c}{d} \right)_i \kappa_{\omega i} du' \quad (15)$$

Values for  $d_i$  are available from Refs. 13–15. The collision half-width (1/cm) for gas  $i$  is given by

$$\gamma_{Ci} = \sum_j (\gamma_{i,j})_{273} Y_j P \left( \frac{273}{T} \right)^{\eta_{i,j}} + (\gamma_{i,i})_{273} Y_i P \left( \frac{273}{T} \right)^{\eta_{i,i}} \quad (16)$$

where the broadening by gas  $j$  is contained in the  $i, j$  terms, and the self-broadening is contained in the  $i, i$  terms. The values for  $\gamma_{i,j}$ ,  $\gamma_{i,i}$ ,  $\eta_{i,j}$ , and  $\eta_{i,i}$  are available (Ref. 13, Table 5.19, p. 223), or from the SRRM database.<sup>14,15</sup>

The total optical thickness  $\tau_\omega$  is

$$\tau_\omega = \sum_i X_i \quad (17)$$

and the Beer's law optical thickness is

$$\tau_\omega^* = \sum_i X_i^* \quad (18)$$

### Numerical Method

The radiative intensity from Eq. (4), assuming cold walls, or that  $I_\omega(\tau_{\omega w}, \theta, \phi) \ll I_B(\omega, T)$ , becomes

$$I_\omega(0, \theta, \phi) = I_B(\omega, T)[1 - \exp(-\tau_{\omega w})] \quad (19)$$

at the combustor wall point located at  $x = x_p$ ,  $y = y_p$ , and  $z = 0$ . In this notation,  $x_p$  and  $y_p$  are dropped for simplicity.

The radiative flux at a specific value of  $\omega$  is calculated by integrating Eq. (6) over the angles  $\theta$  and  $\phi$  using finite differences. The step-sizes are  $\Delta\theta = 90/(i_m - 1)$  and  $\Delta\phi = 360/(j_m - 1)$ . Also the average value of  $\theta$  for the step from  $i$  to  $i + 1$  is  $\bar{\theta} = \theta_i + \Delta\theta/2$ . The integral over  $\theta$  is from  $0 \leq \theta \leq \pi/2$ , because there is no contribution to the radiation for  $\pi/2 \leq \theta \leq \pi$  when  $z_p = 0$ . First, the solid angle integral is done over  $\theta$  at a fixed value of  $\phi(\phi_j)$ , such that

$$F_\omega(0, \phi_j) = \sum_{i=1}^{i_m-1} \frac{1}{2} [I_\omega(0, \phi_j, \theta_i) + I_\omega(0, \phi_j, \theta_{i+1})] \cos \bar{\theta} \sin \bar{\theta} \Delta\theta \quad (20)$$

Next, the integration is done on  $\phi$

$$F_\omega(0) = \sum_{j=1}^{j_m-1} \frac{1}{2} [F_\omega(0, \phi_j) + F_\omega(0, \phi_{j+1})] \Delta\phi \quad (21)$$

The total flux at  $z = 0$  is obtained by evaluating Eq. (21) at each  $\omega$  of interest ( $\omega_k$ , for  $k = 1, k_m$ ) and then summing over  $\omega$ , such that

$$F(0) = \sum_{k=1}^{k_m-1} \frac{1}{2} [F_{\omega_k}(0) + F_{\omega_{k+1}}(0)] \Delta\omega \quad (22)$$

The step sizes used in the numerical calculations were  $\Delta\theta = \Delta\phi = 2$  deg. In other words  $i_m = 46$  and  $j_m = 181$ . The spectral database contained data every 20 1/cm from 400 to 5000 1/cm (wavelengths from 2 to 25  $\mu\text{m}$ ). Thus,  $\Delta\omega = 20$  1/cm, so  $k_m = 231$ , and in Eq. (22)  $\omega_1 = 400$ ,  $\omega_2 = 420$ , etc.

### Radiation Predictions

Calculations have been made to evaluate scramjet radiative heating for  $\text{H}_2$ -air combustion. SPARK solutions for a three-dimensional, full-scale, scramjet combustor at a flight Mach number of 14 with film cooling were one dimensionalized for this radiation analysis. In addition, a one-dimensional cycle-code was used to obtain solutions for a missile configuration, scramjet combustor at flight Mach numbers of 9.77 and 7.67. Two cases are presented for  $M_0 = 7.67$ ; case a for  $\phi = 0.675$  and case b for  $\phi = 0.351$ . The combustor geometry was assumed to be rectangular and the wall temperatures were 1100 K for the Mach 14 case and 1000 K for the other cases. The parameters that describe the combustor flow, given in Table 2, were obtained from calculations in Refs. 10 and 11. The thermodynamic conditions and composition vary along the combustor, thus, the values given in Table 2, and used in the analysis, are average values and are representative of the entire combustor. In other words, the combustors were assumed to have constant properties as listed in Table 2. All of the combustors are multiples of 6.65 cm wide. Note that the Mach 14 combustor is much larger than the others.

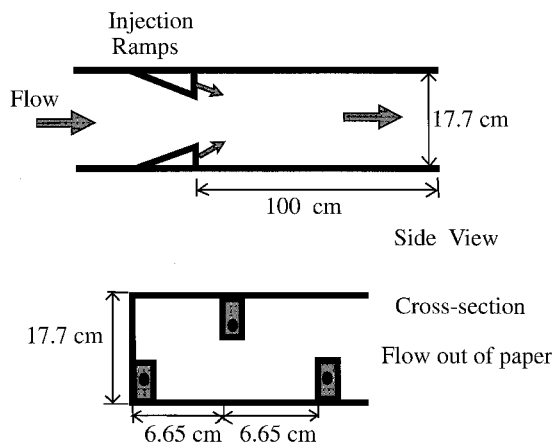
### Convective Heating

A simple estimate of the convective heat transfer rate consists of writing

$$q = St\rho_0 v_0 (h_{\text{aw}} - h_w) \approx St\rho_0 v_0^3/2 \quad (23)$$

**Table 2 Scramjet flowfields**

Parameter	Mach number			
	14	9.77	7.67(a)	7.67(b)
$P_o$ , atm	0.0072	0.01	0.01	0.01
$T_o$ , K	232	200	200	200
$\rho_o$ , kg/m <sup>3</sup>	0.011	0.017	0.076	0.076
$v_o$ , m/s	4274	2800	2200	2200
$\rho_o v_o^3/2$ , W/cm <sup>2</sup>	43,020	19,120	9274	9274
$x_o$ , cm	100	20	20	20
$y_o$ , cm	17.7	3	4.76	4.76
$\phi$	1.5	1.0	0.695	0.351
$T$ , K	2924	3091	2715	1956
$P$ , atm	4.69	8.77	5.68	2.86
$\rho$ , kg/m <sup>3</sup>	0.393	0.811	0.637	0.478
$Y_{H_2O}$	0.205	0.269	0.204	0.110
$Y_{OH}$	0.020	0.029	0.020	0.015
$Y_O$	0.005	0.003	0.003	0.001
$Y_H$	0.190	0.044	0.035	0.017
$Y_{O_2}$	0.025	0.014	0.064	0.128
$Y_H$	0.028	0.016	0.002	0.002
$Y_N$	0.528	0.624	0.672	0.728
$M_w$ , kg/kmol	20.16	23.42	25.00	26.78

**Fig. 3** Schematic of side view and cross-sectional view of a Mach 14, full-scale, scramjet combustor. The injector pattern repeats every 6.65 cm.

where the enthalpy difference is approximated as the free-stream kinetic energy. Values of  $\rho_o v_o^3/2$  are given in Table 2. The Stanton number is a function of many parameters, including Reynolds number, Prandtl number, wall catalytic properties, turbulence, and the ratio of wall-to-gas temperature. Thus, to estimate the convective heat transfer, the Stanton number is assumed to be 0.01.<sup>16</sup> This gives representative convective heat transfer rates of 430, 191, and 93 W/cm<sup>2</sup>, for the  $M_o = 14$ , 9.77, and 7.67 cases, respectively. Values for the convective heat transfer rate for real scramjet combustors are hard to find in the open literature. The heat transfer rate is usually given normalized by a reference value, but the reference value is not given, because much of the data on real systems are classified.<sup>17,18</sup> Consequently, the estimated convective heat transfer rates given previously will be used to compare with the radiative heat transfer rates in this article.

#### Mach 14

For the  $M_o = 14$  case, the average combustor Mach number was 2.756, corresponding to a velocity of 3397 m/s. The full-scale combustion chamber is shown schematically in Fig. 3. Radiation was calculated at the center of the 100-cm wall ( $x_p$ ,  $y_p$ , and  $z_p = 50$ , 8.85, and 0 cm, respectively). The radiative flux was evaluated for three values of combustor width,  $z_o = 6.65$ , 13.3, and 26.6 cm, respectively, to account for multiple sets of injectors. The radiating species were H<sub>2</sub>O and OH.

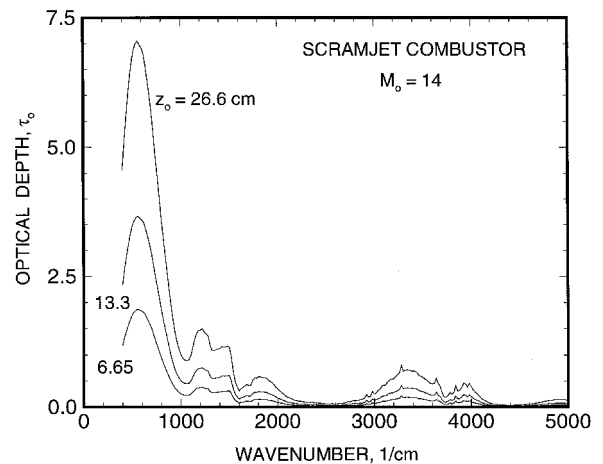
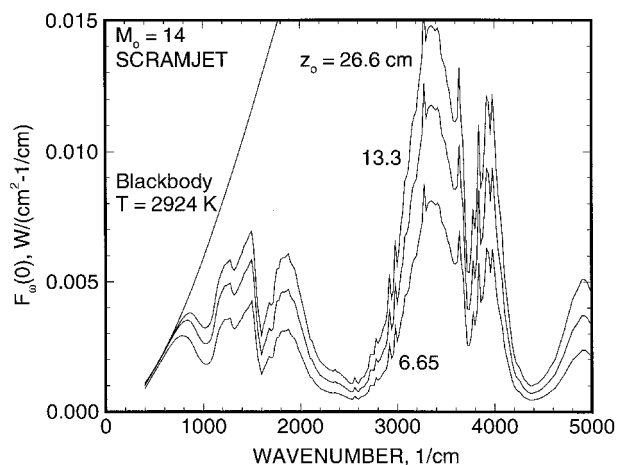
Figure 4 shows the optical depth across the combustor ( $\tau_o = \kappa_o z_o$ ) as a function of  $\omega$  for three  $z_o$  values. The maximum optical depth occurs at  $\omega \approx 600$  1/cm and it is large enough so that self-absorption is important. The values of  $z_o = 13.3$  and 26.6 cm can be thought of as distances along different angular directions, or as widths of larger combustors.

Figure 5 shows the spectral radiative flux as a function of  $\omega$ . The maximum emission occurs in the 2.7- $\mu$ m band of H<sub>2</sub>O and OH at approximately 3300 1/cm. Both gases have bands at this  $\omega$ . The blackbody spectral flux for  $T = 2924$  K is shown for reference.

Figure 6 shows the accumulative radiative flux from 0 to  $\omega$  as a function of  $\omega$ . For instance, for  $z_o = 6.65$  cm, the total flux is 12.5 W/cm<sup>2</sup> for  $\omega$  less than 5000 1/cm. Likewise, it is 5 W/cm<sup>2</sup> for  $\omega$  below 3000 1/cm. Also, the blackbody curve represents the accumulative blackbody flux from 0 to  $\omega$ . This curve quickly goes off scale. The magnitude of radiative heating ranges from 12.5 to 23.4 W/cm<sup>2</sup> for the  $z_o$  considered. These magnitudes of radiative heating are significant and will require some thermal protection.

#### Mach 9.77

For the one-dimensionalized  $M_o = 9.77$  case, the inlet Mach number was 4.012. The thermodynamic conditions and composition are given in Table 2. The major difference between this case and the  $M_o = 14$  case is the roughly doubling of the combustor pressure. Figure 1 shows a schematic of the scramjet-powered vehicle and its combustor. The inlet geometry is such that the oblique shocks are canceled at the combustor

**Fig. 4** Mach 14 scramjet combustor optical depth across width of combustor ( $\kappa_o z_o$ ) as a function of  $\omega$ .**Fig. 5** Mach 14 scramjet combustor radiation flux as a function of  $\omega$ .

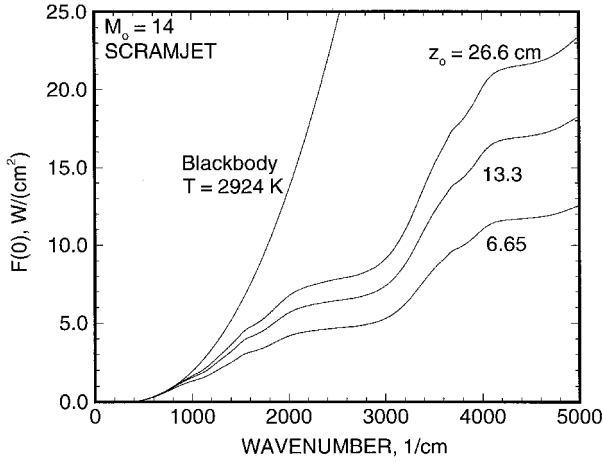


Fig. 6 Mach 14 accumulative combustor radiation flux from  $\omega = 0$  to  $\omega$  as a function of  $\omega$ .

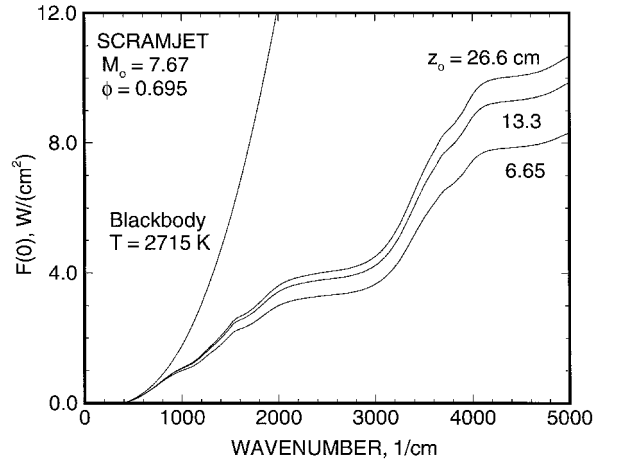


Fig. 8 Mach 7.67(a) scramjet combustor accumulative radiation flux from  $\omega = 0$  to  $\omega$  as a function of  $\omega$ .

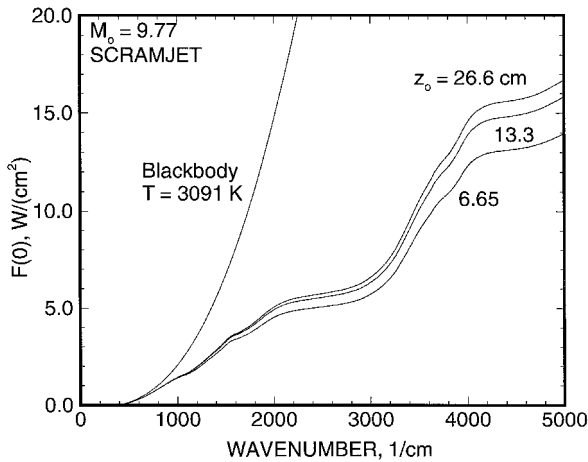


Fig. 7 Mach 9.77 combustor accumulative radiation flux from  $\omega = 0$  to  $\omega$  as a function of  $\omega$ .

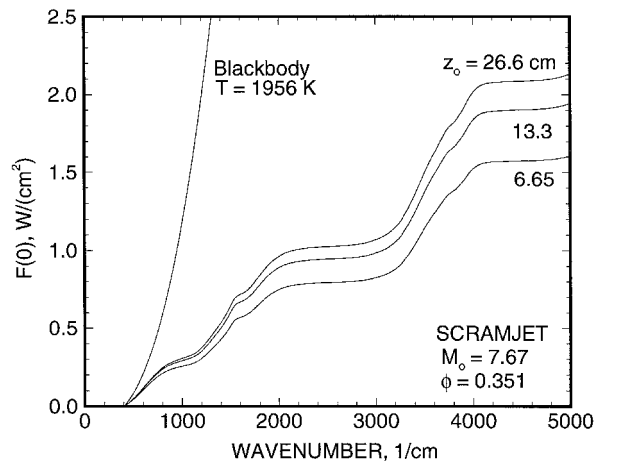


Fig. 9 Mach 7.67(b) scramjet combustor accumulative radiation flux from  $\omega = 0$  to  $\omega$  as a function of  $\omega$ .

entrance. The radiation calculations are for the point at  $(x_p, y_p, z_p) = (10, 1.5, 0)$ . The optical depth is about twice as large as the optical depth for the  $M_0 = 14$  case because of the doubling of the pressure. Self-absorption is important near 600 1/cm.

Figure 7 shows the integrated radiative flux from 0 to  $\omega$  as a function of  $\omega$ . At  $z_0 = 6.65$  cm, the total flux is 14 W/cm<sup>2</sup> for  $\omega$  less than 5000 1/cm. Likewise, it is about 6.5 W/cm<sup>2</sup> for  $\omega$  below 3000 1/cm. The large increase between 3000–4000 1/cm is caused by the emission from the 2.7- $\mu$ m band of H<sub>2</sub>O and OH. The magnitude of radiative heating ranges from 14 to 16.7 W/cm<sup>2</sup> for this analysis. Radiative heating is significant and will require some thermal protection.

#### Mach 7.67(a), $\phi = 0.695$

For the  $M_0 = 7.67$  case the inlet Mach number was 3.497. Pressure and the mole fractions for this case are about the same as they were for the  $M_0 = 14$  case; however,  $T$  is 7% lower because of the lower  $\phi$ . The exit Mach number was 1.12. The radiation calculations are for the point at  $(x_p, y_p, z_p) = (10, 2.38, 0)$ .

Figure 8 shows the accumulative radiative flux from 0 to  $\omega$  as a function of  $\omega$ . For  $z_0 = 6.65$  cm, the total flux is about 8 W/cm<sup>2</sup> for  $\omega$  less than 5000 1/cm and about 3 W/cm<sup>2</sup> for  $\omega$  below 3000 1/cm. The radiative heating is significant and will require some thermal protection.

#### Mach 7.67(b), $\phi = 0.351$

For this  $M_0 = 7.67$  case the inlet Mach number was 3.497 and the exit Mach number was 1.78. This case differs from

the previous one because of its lower  $\phi$  value; it is more fuel-lean.  $Y_{H_2O}$ ,  $Y_{OH}$ ,  $T$ , and  $P$  are all much lower than they were for the other cases. The thermodynamic conditions and composition are listed in Table 2. The calculations are for the point at  $(x_p, y_p, z_p) = (10, 2.38, 0)$ .

Figure 9 shows the integrated radiative flux from 0 to  $\omega$  as a function of  $\omega$ . For  $z_0 = 6.65$  cm, the total flux is about 1.6 W/cm<sup>2</sup> for  $\omega$  less than 5000 1/cm. The magnitude of radiative heating ranges from 1.6 to 2.1 W/cm<sup>2</sup> for this case, and is much less than it was for the  $\phi = 0.695$  case because of lower temperature and lower  $Y_{H_2O}$ . The radiative heating is not significant for this case.

Table 3 summarizes the radiative flux that reaches the mid-point of the  $z = 0$  wall of the combustors. The predicted radiative flux values are in general agreement with the gas turbine combustor radiation measurements of Rosfjord.<sup>19</sup> The radiative heating is important for values above 10 W/cm<sup>2</sup>; thus, some thermal protection will be necessary for scramjet combustors used in hypersonic aircraft, where many long flights occur between inspections. These radiation fluxes should be compared to the estimated convective heat transfer rates discussed earlier, which were 430, 191, and 93 W/cm<sup>2</sup> for the  $M_0 = 14, 9.77$ , and 7.67 cases, respectively. The radiative heating is of the order of 10% of the total heating.

This study shows that radiative flux can be significant. Considering additional bands and gases (like NO) will increase the radiation. Its magnitude can reach 10–25 W/cm<sup>2</sup>, which, when combined with the convective heating of the order of 100–400 W/cm<sup>2</sup>, will require additional thermal insulation to pro-

**Table 3 Scramjet radiation flux, W/cm<sup>2</sup>**

Mach number	$z_o = 6.65$	$z_o = 13.30$	$z_o = 26.60$
14	12.54	18.28	23.40
9.77	13.96	15.83	16.71
7.67(a)	8.31	9.87	10.69
7.67(b)	1.61	1.94	2.13

tect the wall. The radiation heating is about 10% of the convective heating. The predicted radiative flux magnitudes generally agree with those predicted by Liu and Tiwari.<sup>5</sup> It is necessary to keep the wall temperatures on the order of 1000 K because of the material properties, and so radiative heating appears to be an important problem and needs further investigation.

The maximum combustor width considered in this study is 26.6 cm. This dimension is smaller than some of the current engine designs and test rigs. For larger widths the radiative heating will increase, owing to larger optical depths. For wide combustors it may be necessary to use splitter plates to isolate a bank of injector modules to control the magnitude of the radiative heating.

### Conclusions

A simple, preliminary analysis of the radiative transfer in scramjet combustors has been presented. The radiation emission from H<sub>2</sub>O and OH molecules in the flow was calculated. If other gases are considered, the radiation heating will increase. Realistic thermal environments were considered. The radiative heating is significant for full-scale combustors. It is about 10% of the convective heating. The combustor walls will require heat-shielding liners to withstand the heat loads, especially for airplane applications. Larger combustors will have larger radiative heating.

### Acknowledgment

The author wishes to acknowledge many helpful discussions with David W. Riggins.

### References

- <sup>1</sup>Scott, W. B., "USAF, NASA Programs to Push Hypersonic Boundaries," *Aviation Week and Space Technology*, May 6, 1996, pp. 22, 23.
- <sup>2</sup>Riggins, D. W., McClinton, C. R., Rogers, R. C., and Bittner, R. D., "Investigation of Scramjet Injection Strategies for High Mach Number Flow," *Journal of Propulsion and Power*, Vol. 11, No. 3,

1995, pp. 409–418.

<sup>3</sup>Kandebo, S. W., "Scramjet Test Bridges Hypersonic Efforts," *Aviation Week and Space Technology*, March 28, 1994, pp. 52–54.

<sup>4</sup>Cambier, J.-L., Adelman, H. G., and Menees, G. P., "Numerical Simulations of Oblique Detonations in Supersonic Combustion Chambers," *Journal of Propulsion and Power*, Vol. 5, No. 4, 1988, pp. 482–491.

<sup>5</sup>Liu, J., and Tiwari, S. N., "Radiative Interactions in Chemically Reacting Compressible Nozzle Flows Using Monte Carlo Simulations," AIAA Paper 94-2092, June 1994.

<sup>6</sup>Drummond, J. P., Rogers, R. C., and Hussaini, M. Y., "A Detailed Numerical Model of a Supersonic Reacting Mixing Layer," AIAA Paper 86-1427, June 1986.

<sup>7</sup>Drummond, J. P., Carpenter, M. H., and Riggins, D. W., "Mixing and Mixing Enhancement in Supersonic Reacting Flowfields," *High Speed Flight Propulsion Systems*, edited by S. N. B. Murthy and E. T. Curran, Vol. 137, Progress in Astronautics and Aeronautics, AIAA, Washington, DC, 1991, pp. 383–455.

<sup>8</sup>Singh, D. J., Carpenter, M. H., and Kumar, A., "Numerical Simulation of Shock-Induced Combustion/Detonation in a Premixed H<sub>2</sub>/Air Mixture Using Navier-Stokes Equations," AIAA Paper 91-3359, June 1991.

<sup>9</sup>Carpenter, M. H., "Three-Dimensional Computations of Cross-Flow Injection and Combustion in a Supersonic Flow," AIAA Paper 89-1870, June 1989.

<sup>10</sup>Riggins, D. W., and McClinton, C., "Thrust Modeling for Hypersonic Engines," AIAA Paper 95-6081, April 1995.

<sup>11</sup>Riggins, D. W., "The Evaluation of Performance Losses in Multi-Dimensional Flows," AIAA Paper 96-0375, Jan. 1996.

<sup>12</sup>Ozisik, M. N., *Radiative Transfer and Interactions with Conduction and Convection*, Wiley, New York, 1973, Chap. 8.

<sup>13</sup>Ludwig, C. B., Malkmus, W., Reardon, J. E., and Thompson, J. A. L., "Handbook of Infrared Radiation from Combustion Gases," NASA SP-3080, 1973.

<sup>14</sup>Ludwig, C. B., Malkmus, W., Walker, J., Freeman, G. N., Reed, R. A., and Slack, M., "Standardized Infrared Radiation Model (SIRRM)," Air Force Rocket Propulsion Lab., TR-81-54, Edwards AFB, CA, Aug. 1981.

<sup>15</sup>Ludwig, C. B., Malkmus, W., Walker, J., Freeman, G. N., Slack, M., and Reed, R. A., "A Theoretical Model for Absorbing, Emitting and Scattering Plume Radiation," *Spacecraft Radiative Transfer and Temperature Control*, edited by T. E. Horton, Vol. 83, Progress in Astronautics and Aeronautics, AIAA, New York, 1982, pp. 111–127.

<sup>16</sup>Tauber, M. E., "A Review of High-Speed, Convective, Heat-Transfer Methods," NASA TP 2914, July 1989.

<sup>17</sup>Kamath, P. S., Mao, M. M., and McClinton, C. R., "Scramjet Combustor Analysis with the Ship3D PNS Code," AIAA Paper 91-5090, Dec. 1991.

<sup>18</sup>Bobskill, G. J., Bittner, R. D., Riggins, D. W., and McClinton, C. R., "CFD Evaluation of Mach 17 HYPULSE Scramjet Combustion Data," AIAA Paper 91-5093, Dec. 1991.

<sup>19</sup>Rosfjord, T. J., "Role of Fuel Chemical Properties on Combustor Radiative Heat Load," *Journal of Propulsion and Power*, Vol. 3, No. 6, 1987, pp. 494–501.